NASA TECHNICAL NOTE

NASA TN D-2421

NASA TN D-2421

HEAT TRANSFER FOR LAMINAR SLIP FLOW OF A RAREFIED GAS BETWEEN PARALLEL PLATES WITH UNSYMMETRICAL WALL HEAT FLUX

by Robert M. Inman

Lewis Research Center
Cleveland, Ohio

NATIONAL AERONAUTICS AND SPACE ADMINISTRATION • WASHINGTON, D. C. • AUGUST 1964

HEAT TRANSFER FOR LAMINAR SLIP FLOW OF A RAREFIED GAS BETWEEN PARALLEL PLATES WITH UNSYMMETRICAL WALL HEAT FLUX

By Robert M. Inman

Lewis Research Center
Cleveland, Ohio

NATIONAL AERONAUTICS AND SPACE ADMINISTRATION

For sale by the Office of Technical Services, Department of Commerce,
Washington, D.C. 20230 -- Price $1.00

HEAT TRANSFER FOR LAMINAR SLIP FLOW OF A RAREFIED GAS BETWEEN PARALLEL PLATES WITH UNSYMMETRICAL WALL HEAT FLUX

by Robert M. Inman

Lewis Research Center

SUMMARY

An analysis has been made to determine the effects of low-density phenomena on the forced convection heat-transfer characteristics for fully developed laminar flow in a parallel plate channel for unsymmetrical heating involving a constant heat flux along each of the walls. Consideration is given to the slip-flow regime wherein the major rarefaction effects are manifested as velocity and temperature jumps at the channel walls. The results obtained apply along the entire length of the channel. The solution contains series expansions, and analytical expressions for the complete sets of eigenvalues and eigenfunctions are presented. The results give the wall temperatures and the thermal entrance lengths for the channel for various mean free paths and wall heat flux ratios. The results indicate that, in general, the thermal entrance length is decreased with increasing gas rarefaction and also that for a given mean free path the thermal entrance length is greater for unsymmetrical heating than for a symmetrical wall heat flux. Extension of the results is made or indicated to account for less frequently considered slip effects such as wall shear work, modified temperature jump, and thermal creep velocity.

INTRODUCTION

The heating and cooling of gases flowing inside ducts are among the most important heat-transfer processes in engineering. The design and analysis of compact heat exchange equipment, for example, requires a knowledge of the duct wall temperatures. Asymmetric heating or cooling is often encountered when dealing with forced convection heat transfer for gas flow through flat rectangular ducts. In a compact heat exchanger, for instance, the core very often consists of stacks of rectangular passages through which a gas flows. In the outermost passage of the exchanger core, the gas flows between a plate and the unheated structure which may be insulated from the outside environment. Other examples of instances when this situation may arise are (1) when different coolants are employed in adjacent flow channels, so that the sandwiched gas experiences unequal heat addition or removal at its channel walls; (2) when the temperature of the environment at one side differs from that at the other side of the channel, so that unequal wall heat fluxes exist; or (3) when heat leakage or addition through insulation occurs.

An increasingly important engineering problem is that of predicting heat-transfer characteristics of slightly rarefied gases flowing inside ducts. Under the conditions of high-altitude flight, for example, the gas flow inside a flat duct may be sufficiently rarefied so that the appropriate mean free path becomes too large for the application of continuum transfer equations but not large enough for free-molecule or transition concepts to apply. In this flow regime of slight gas rarefaction, termed the slip-flow regime, the gas density is slightly less than that characteristic of a continuum flow. At this slightly reduced density, the gas adjacent to a solid surface will have a velocity and temperature different from those of the surface. The effects on the heat-transfer conditions in channels of these low-density phenomena, combined with unsymmetrical heating or cooling situations, are of practical interest to the design engineer.

The case of laminar continuum flow between parallel flat plates with different temperatures prescribed along each of the two walls has been considered in references 1 to 3. The case of laminar continuum flow between parallel flat plates with unsymmetrically prescribed heat flux at the walls has been investigated in reference 4.

Heat transfer for laminar slip flow of a rarefied gas in a parallel plate channel has been studied for uniform wall heat flux (ref. 5). The results allow for either equal heating at both walls or heating one wall and insulating at the other.

The present investigation is concerned with the heat transfer for laminar slip flow of a rarefied gas between parallel plates with constant but unequal heat fluxes specified at the walls. Flow through a flat rectangular duct may be expected to approximate the flow between parallel plates if one side of the rectangle is large compared with the other, the heat fluxes being perpendicular to the long side. In addition, the results are expected to apply for annuli where the radius ratio is close to unity.

The present analysis requires the calculation of the odd eigenvalues and constants for laminar slip flow of a rarefied gas, such that the complete solution is obtained by combining these odd quantities with the even eigenvalues and constants that have been determined in reference 5 for a symmetrically prescribed uniform wall heat flux.

In the main body of the investigation, the effects of velocity-slip and temperature-jump boundary conditions are studied. In the final section of the investigation, modification of the heat-transfer results will be made or discussed to account for the effects of wall shear work, modified temperature jump, and thermal creep velocity.

ANALYSIS

A schematic diagram of the system under study is pictured in figure 1,

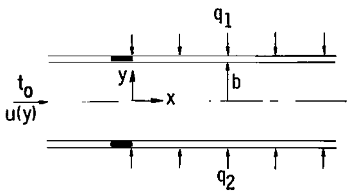

Figure 1. - Physical model and coordinate system.

which also shows dimensions and coordinates. The direction of the gas flow is from left to right. The flow is assumed to be laminar, incompressible, and fully developed. The fully developed velocity distribution for slip flow in a parallel plate channel has been considered in reference 5, and the results are used in the present investigation. For $x < 0$ the channel walls and gas are isothermal at temperature t_0, whereas for $x \geq 0$ the constant heat fluxes (per unit surface area) q_1 and q_2 are applied at the upper and lower walls, respectively. These fluxes are taken as positive when the gas is being heated. It is desired to determine the temperature distributions along the entire length of the channel.

Energy Equation

The energy equation for the channel illustrated in figure 1 can be written as

$$u \frac{\partial t}{\partial x} = \alpha \frac{\partial^2 t}{\partial y^2} \tag{1}$$

The gas properties have been assumed constant, and viscous dissipation and axial conduction have been neglected compared with conduction in the transverse y-direction. The boundary conditions are

Specified wall heat flux:

$$\frac{\partial t}{\partial y} = \frac{q_1}{\kappa} \qquad \text{at} \quad y = +b, \; x \geq 0 \tag{2a}$$

Specified wall heat flux:

$$\frac{\partial t}{\partial y} = - \frac{q_2}{\kappa} \qquad \text{at} \quad y = -b, \; x \geq 0 \tag{2b}$$

Specified entrance temperature:

$$t = t_0 \qquad \text{at} \quad x = 0 \tag{2c}$$

The slip-flow velocity distribution is given in reference 5 as

$$\frac{u(\eta)}{\bar{u}} = f(\eta) = \frac{3}{2} \frac{(1 - \eta^2 + 4\theta)}{1 + 6\theta} \tag{3a}$$

$$\frac{u_s}{\bar{u}} = f(1) = \frac{6\theta}{1 + 6\theta} \tag{3b}$$

where $\theta \equiv \xi_u/2b$. The slip coefficient ξ_u is given by the expression (ref. 6)

$$\xi_u = \frac{2 - g}{g} l \tag{4}$$

where g is the specular reflection coefficient and l is the mean free path,

$$l = \sqrt{\frac{\pi}{2}} \frac{\mu\sqrt{R_g t}}{p} \tag{5}$$

Equations (1) and (2) may be expressed in terms of nondimensional quantities as

$$f(\eta) \frac{\partial t}{\partial \zeta} = \frac{\partial^2 t}{\partial \eta^2} \tag{6}$$

$$\frac{\partial t}{\partial \eta} = \frac{q_1 b}{\kappa} \qquad \text{at} \quad \eta = 1 \tag{7a}$$

$$\frac{\partial t}{\partial \eta} = -\frac{q_2 b}{\kappa} \qquad \text{at} \quad \eta = -1 \tag{7b}$$

$$t = t_0 \qquad \text{at} \quad \zeta = 0 \tag{7c}$$

To obtain a solution for t that will apply over the entire length of the channel, it is convenient to break t into two parts. The first part is t_d, the fully developed solution, which applies far down the channel from the entrance. The second part is t_e, which is an entrance region solution that is added to t_d to obtain temperatures in the region near the entrance of the channel. The temperatures throughout the channel are given by

$$t = t_d + t_e \tag{8}$$

Fully Developed Solution

Far from the entrance of the channel the temperature rises linearly in the axial direction because of the uniform (but unequal) heat inputs at the channel walls. From a heat balance on the gas, the temperature gradient in the fully developed region must be

$$\frac{\partial t_d}{\partial \zeta} = \text{const} = \frac{(q_1 + q_2)b}{2\kappa} \tag{9}$$

For the fully developed situation the boundary condition at the entrance of the heated channel $(x = 0)$ need not be considered, since it is accounted for by the entrance region solution, and equation (9) may be rephrased as

$$\frac{t_d - t_0}{\frac{(q_1 + q_2)b}{2\kappa}} = \frac{4\frac{x}{2b}}{RePr} + H(\eta) \tag{10}$$

The function $H(\eta)$ is found by inserting equation (10) into the differential equation (6). This leads to the equation for $H(\eta)$ as

$$\frac{d^2H}{d\eta^2} = f(\eta) \tag{11}$$

The boundary conditions on $H(\eta)$ are determined from the boundary conditions on t_d, so that

$$\frac{dH}{d\eta} = \frac{(q_1 b)(2\kappa)}{(q_1 + q_2)b\kappa} \qquad \text{at} \quad \eta = 1 \tag{12a}$$

$$\frac{dH}{d\eta} = -\frac{(q_2 b)(2\kappa)}{(q_1 + q_2)b\kappa} \qquad \text{at} \quad \eta = -1 \tag{12b}$$

Consideration of an overall energy balance on the gas for the length of channel from 0 to x produces the additional condition on $H(\eta)$

$$\int_{-1}^{+1} H(\eta)f(\eta)d\eta = 0 \tag{12c}$$

Equation (11) can be integrated directly. The resulting expression for t_d is

$$\frac{t_d - t_0}{\frac{(q_1 + q_2)b}{2\kappa}} = \left[\frac{4\frac{x}{2b}}{RePr} + \frac{3}{4}\eta^2 - \frac{1}{8}\eta^4 - \frac{39}{280} + \frac{\eta(q_1 - q_2)}{q_1 + q_2}\right] + \frac{u_s}{\bar{u}}\left(-\frac{1}{4}\eta^2 + \frac{1}{8}\eta^4 - \frac{13}{280}\right) + \left(\frac{u_s}{\bar{u}}\right)^2 \frac{2}{105} \tag{13}$$

The quantity in the first bracket on the right side of equation (13) represents the customary transverse temperature distribution for continuum flow conditions (ref. 4), while the quantities in parentheses are connected with the effect of the velocity jump. Equation (13) applies only in the fully developed region downstream of the thermal entrance region.

Entrance Region

To determine the solution in the thermal entrance region the function t_e is needed. The function t_e must satisfy the equation

$$f(\eta)\,\frac{\partial t_e}{\partial \zeta} = \frac{\partial^2 t_e}{\partial \eta^2} \tag{14}$$

with the boundary conditions

$$\frac{\partial t_e}{\partial \eta} = 0 \qquad \text{at} \quad \eta = -1 \quad \text{and} \quad \text{at} \quad \eta = +1 \tag{15a}$$

At $x = 0$, the condition is

$$t(0,\eta) = t_0 = t_d(0,\eta) + t_e(0,\eta)$$

or by rearranging,

$$t_e(0,\eta) = -\left[t_d(0,\eta) - t_0\right] \tag{15b}$$

It will be convenient to represent the entrance temperature t_e by two functions, $\Phi(\zeta,\eta)$ and $\Omega(\zeta,\eta)$, such that (ref. 4)

$$\frac{t_e}{\frac{(q_1 + q_2)b}{2\kappa}} = \Phi + \left(\frac{q_1 - q_2}{q_1 + q_2}\right)\Omega \tag{16}$$

By substituting equation (16) into equation (14), it is found that the function Φ is given by

$$f(\eta)\,\frac{\partial \Phi}{\partial \zeta} = \frac{\partial^2 \Phi}{\partial \eta^2} \tag{17a}$$

with the boundary conditions

$$\frac{\partial \Phi}{\partial \eta} = 0 \qquad \text{at} \quad \eta = -1 \quad \text{and} \quad \eta = +1 \tag{17b}$$

and the function Ω is given by

$$f(\eta)\,\frac{\partial \Omega}{\partial \zeta} = \frac{\partial^2 \Omega}{\partial \eta^2} \tag{18a}$$

with the boundary conditions

$$\frac{\partial \Omega}{\partial \eta} = 0 \qquad \text{at} \quad \eta = -1 \quad \text{and} \quad \eta = +1 \tag{18b}$$

The condition at $\zeta = 0$ will be discussed shortly.

A solution to equation (17a) can be obtained as a product of two functions, one depending on ζ alone, the other depending on η alone. Then it can be shown that Φ is expressed by the series

$$\Phi(\zeta,\eta) = \sum_{n=1}^{\infty} a_n Y_n(\eta)\exp\left(\frac{-4\lambda_n \frac{x}{2b}}{RePr}\right) \tag{19}$$

where λ_n and Y_n are, respectively, the eigenvalues and eigenfunctions of the Sturm-Liouville problem

$$\left.\begin{aligned} &\frac{d^2Y_n}{d\eta^2} + \lambda_n f(\eta)Y_n = 0 \\ &\frac{dY_n}{d\eta} = 0 \qquad \text{at} \quad \eta = -1 \quad \text{and} \quad \eta = +1 \end{aligned}\right\} \tag{20}$$

In a similar manner, the function Ω is expressed by the series

$$\Omega(\zeta,\eta) = \sum_{n=0}^{\infty} b_n Z_n(\eta)\exp\left(\frac{-4\gamma_n \frac{x}{2b}}{RePr}\right) \tag{21}$$

where γ_n and Z_n are, respectively, the eigenvalues and eigenfunctions of the Sturm-Liouville problem

$$\left.\begin{aligned} &\frac{d^2Z_n}{d\eta^2} + \gamma_n f(\eta)Z_n = 0 \\ &\frac{dZ_n}{d\eta} = 0 \qquad \text{at} \quad \eta = -1 \quad \text{and} \quad \eta = +1 \end{aligned}\right\} \tag{22}$$

Combining equations (19) and (21) in accordance with equation (16) yields the entrance temperature as

$$\frac{t_e}{\frac{(q_1 + q_2)b}{2\kappa}} = \sum_{n=1}^{\infty} a_n Y_n(\eta)\exp\left(\frac{-4\lambda_n \frac{x}{2b}}{RePr}\right) + \frac{q_1 - q_2}{q_1 + q_2}\sum_{n=0}^{\infty} b_n Z_n(\eta)\exp\left(\frac{-4\gamma_n \frac{x}{2b}}{RePr}\right) \tag{23}$$

The coefficients a_n in equation (19) and b_n in equation (21) are evaluated to satisfy the condition at the entrance to the heated channel ($x = 0$).

Evaluating equations (13) and (23) at $x = 0$ and substituting the values into equation (15b) gives

$$\sum_{n=1}^{\infty} a_n Y_n(\eta) + \frac{q_1 - q_2}{q_1 + q_2} \sum_{n=0}^{\infty} b_n Z_n(\eta) = -\left[\frac{3}{4}\eta^2 - \frac{1}{8}\eta^4 - \frac{39}{280}\right.$$

$$\left. + \frac{q_1 - q_2}{q_1 + q_2}\eta + \frac{u_s}{\bar{u}}\left(-\frac{1}{4}\eta^2 + \frac{1}{8}\eta^4 - \frac{13}{280}\right) + \left(\frac{u_s}{\bar{u}}\right)^2 \frac{2}{105}\right] \tag{24}$$

It is desirable to evaluate a_n and b_n such that

$$\sum_{n=1}^{\infty} a_n Y_n(\eta) = -\left[\frac{3}{4}\eta^2 - \frac{1}{8}\eta^4 - \frac{39}{280} + \frac{u_s}{\bar{u}}\left(-\frac{1}{4}\eta^2 + \frac{1}{8}\eta^4 - \frac{13}{280}\right)\right.$$

$$\left. + \left(\frac{u_s}{\bar{u}}\right)^2 \frac{2}{105}\right] \equiv -G\left(\eta, \frac{u_s}{\bar{u}}\right) \tag{25}$$

$$\sum_{n=0}^{\infty} b_n Z_n(\eta) = -\eta \tag{26}$$

By inspection of equations (25) and (26), it is evident that $Y_n(\eta)$ and $Z_n(\eta)$ are even and odd functions, respectively; that is, $Y_n(\eta) = Y_n(-\eta)$ and $Z_n(\eta) = -Z_n(-\eta)$. According to the Sturm-Liouville theory, the coefficients a_n and b_n are given by the results

$$a_n = -\frac{\int_0^1 G\left(\eta, \frac{u_s}{\bar{u}}\right) f(\eta) Y_n(\eta) d\eta}{\int_0^1 f(\eta) Y_n^2(\eta) d\eta} \tag{27}$$

$$b_n = -\frac{\int_{-1}^1 \eta f(\eta) Z_n(\eta) d\eta}{\int_{-1}^1 f(\eta) Z_n^2(\eta) d\eta} \tag{28}$$

In reference 5 it is shown that the result for the coefficients a_n reduces to

$$a_n = \frac{1}{\left[\lambda\left(\frac{\partial^2 Y}{\partial\eta\ \partial\lambda}\right)\right]_{\eta=1,\lambda=\lambda_n}} \tag{29}$$

The integral appearing in the denominator of equation (28) may be written as

$$\int_{-1}^{1} f(\eta)Z_n^2(\eta)d\eta = -2Z_n(1)\left(\frac{\partial^2 Z_n}{\partial\gamma\ \partial\eta}\right)_{\eta=1,\gamma=\gamma_n}$$

whereas upon substitution of equation (22) and integration by parts the numerator of equation (28) becomes

$$\int_{-1}^{1} \eta f(\eta)Z_n(\eta)d\eta = \frac{2Z_n(1)}{\gamma_n}$$

The series coefficients b_n are thus

$$b_n = \frac{1}{\left[\gamma\left(\frac{\partial^2 Z}{\partial\eta\ \partial\gamma}\right)\right]_{\eta=1,\gamma=\gamma_n}} \tag{30}$$

The functions Y_n and Z_n and the corresponding eigenvalues λ_n and γ_n are as yet undetermined. Nevertheless, before a discussion of the calculation of these quantities is undertaken, the analysis will be extended to the formulation of several quantities of engineering interest.

Now that t_d and t_e are known, they can be superposed as in equation (8) to obtain the solution that applies over the entire length of the channel, which is

$$\frac{t - t_0}{\frac{(q_1 + q_2)b}{2\kappa}} = \frac{4\frac{x}{2b}}{RePr} + G\left(\eta, \frac{u_s}{\bar{u}}\right) + \sum_{n=1}^{\infty} a_n Y_n(\eta)\exp\left(\frac{-4\lambda_n\frac{x}{2b}}{RePr}\right)$$
$$+ \frac{q_1 - q_2}{q_1 + q_2}\left[\eta + \sum_{n=0}^{\infty} b_n Z_n(\eta)\exp\left(\frac{-4\gamma_n\frac{x}{2b}}{RePr}\right)\right] \tag{31}$$

Wall Temperatures

When the wall heat fluxes are specified, the wall temperatures are the unknown quantities that are usually of most practical interest. Before the wall temperature variations can be determined, however, it is necessary to consider another effect of gas rarefaction that enters through the thermal boundary condition at a wall, permitting a jump between the surface temperature t_w and the adjacent gas temperature t_g (ref. 6)

$$t_{g,1} - t_{w,1} = -\xi_t\left(\frac{\partial t}{\partial y}\right)_{y=b} = -2\,\frac{\xi_t}{2b}\left(\frac{\partial t}{\partial \eta}\right)_{\eta=1} \tag{32a}$$

$$t_{g,2} - t_{w,2} = 2\,\frac{\xi_t}{2b}\left(\frac{\partial t}{\partial \eta}\right)_{\eta=-1} \tag{32b}$$

where ξ_t represents a temperature-jump coefficient related to other properties of the system by

$$\xi_t = \frac{2 - a}{a}\,\frac{2\sigma}{\sigma + 1}\,\frac{l}{Pr} \tag{33}$$

Since the wall heat flux is uniform,

$$\left(\frac{\partial t}{\partial \eta}\right)_{\eta=1} = \frac{q_1 b}{\kappa},\quad \left(\frac{\partial t}{\partial \eta}\right)_{\eta=-1} = \frac{-q_2 b}{\kappa}$$

so that the temperature jump at the walls can be written as

$$t_{g,1} - t_{w,1} = -4\,\frac{(q_1 + q_2)b}{2\kappa}\,\frac{q_1}{q_1 + q_2}\,\frac{\xi_t}{2b} \tag{34a}$$

$$t_{g,2} - t_{w,2} = -4\,\frac{(q_1 + q_2)b}{2\kappa}\,\frac{q_2}{q_1 + q_2}\,\frac{\xi_t}{2b} \tag{34b}$$

Then the wall temperatures $t_{w,1}$ and $t_{w,2}$ can be found by evaluating equation (31) at $\eta = 1$ and at $\eta = -1$ and combining the results with equations (34a) and (34b)

$$\frac{t_{w,1} - t_0}{\frac{(q_1 + q_2)b}{2\kappa}} = \frac{4\frac{x}{2b}}{RePr} + \frac{17}{35} - \frac{6}{35}\,\frac{u_s}{\bar{u}} + \frac{2}{105}\left(\frac{u_s}{\bar{u}}\right)^2 + 4\,\frac{q_1}{q_1 + q_2}\,\frac{\xi_t}{2b}$$

$$+ \sum_{n=1}^{\infty} a_n Y_n(1)\exp\left(\frac{-4\lambda_n \frac{x}{2b}}{RePr}\right) + \frac{q_1 - q_2}{q_1 + q_2}\left[1 + \sum_{n=0}^{\infty} b_n Z_n(1)\exp\left(\frac{-4\lambda_n \frac{x}{2b}}{RePr}\right)\right] \tag{35}$$

$$\frac{t_{w,2} - t_0}{\frac{(q_1 + q_2)b}{2\kappa}} = \frac{4\frac{x}{2b}}{\text{RePr}} + \frac{17}{35} - \frac{6}{35}\frac{u_s}{\bar{u}} + \frac{2}{105}\left(\frac{u_s}{\bar{u}}\right)^2$$

$$+ 4\frac{q_2}{q_1 + q_2}\frac{\xi_t}{2b} + \sum_{n=1}^{\infty} a_n Y_n(1)\exp\left(\frac{-4\lambda_n\frac{x}{2b}}{\text{RePr}}\right)$$

$$- \frac{q_1 - q_2}{q_1 + q_2}\left[1 + \sum_{n=0}^{\infty} b_n Z_n(1)\exp\left(\frac{-4\gamma_n\frac{x}{2b}}{\text{RePr}}\right)\right] \tag{36}$$

Convenient alternate forms of equations (35) and (36) are to divide the local wall to bulk temperature difference by the fully developed value. The resulting ratio will then approach unity for large distances from the channel entrance. The ratio is formed as follows: The local bulk gas temperature along the channel is given by

$$\frac{t_b - t_0}{\frac{(q_1 + q_2)b}{2\kappa}} = \frac{4\frac{x}{2b}}{\text{RePr}} \tag{37}$$

Then the difference between the fully developed wall and bulk temperatures for each wall is

$$\frac{(t_{w,1} - t_b)_d}{\frac{(q_1 + q_2)b}{2\kappa}} = \frac{17}{35} - \frac{6}{35}\frac{u_s}{\bar{u}} + \frac{2}{105}\left(\frac{u_s}{\bar{u}}\right)^2 + \frac{q_1 - q_2}{q_1 + q_2} + 4\frac{q_1}{q_1 + q_2}\frac{\xi_t}{2b} \tag{38}$$

$$\frac{(t_{w,2} - t_b)_d}{\frac{(q_1 + q_2)b}{2\kappa}} = \frac{17}{35} - \frac{6}{35}\frac{u_s}{\bar{u}} + \frac{2}{105}\left(\frac{u_s}{\bar{u}}\right)^2 - \frac{q_1 - q_2}{q_1 + q_2} + 4\frac{q_2}{q_1 + q_2}\frac{\xi_t}{2b} \tag{39}$$

To illustrate the results, fully developed wall to bulk temperature differences have been computed as functions of the rarefaction parameter $\mu\sqrt{R_g t}/2pb$, related to the mean free path through equation (5), $\mu\sqrt{R_g t}/2pb = \sqrt{2/\pi}(l/2b)$, for gases with a Prandtl number of 0.73 and a specific heat ratio of 1.4 and for several values of the heat-flux ratio q_2/q_1. For $q_2/q_1 = -1$, the heat addition at the upper wall is equal to the heat extraction at the lower wall. The case for which the lower wall is insulated is represented by $q_2/q_1 = 0$, whereas symmetrical heating corresponds to $q_2/q_1 = 1$. The slip parameter ξ_u was taken from equations (4) and (5) with $g = 1$; while ξ_t was taken from equations (5) and (33) for values of the accommodation coefficient of 1.0 and 0.4. The temperature differences thus obtained have been plotted in figure 2. As gas rarefaction increases, the temperature difference

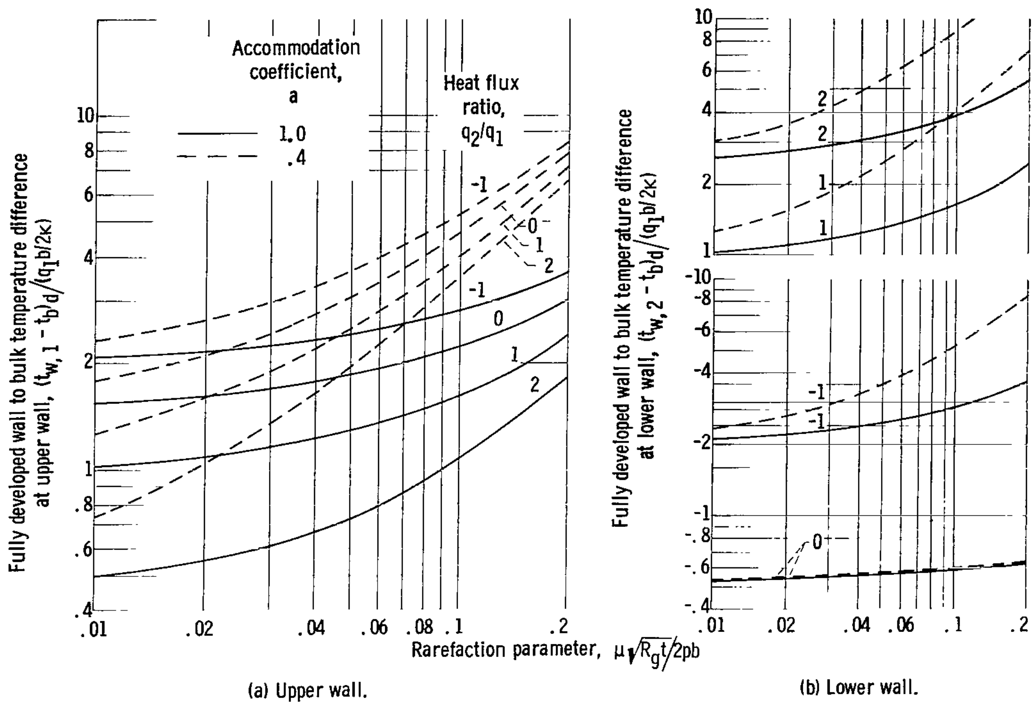

Figure 2. - Fully developed wall to bulk temperature difference. Specular reflection coefficient, 1; specific heat ratio, 1.4; Prandtl number, 0.73.

$(t_{w,1} - t_b)_d$, for a given heat flux ratio, increases over its continuum value, obtained by setting $u_s/\bar{u}$ and $\xi_t/2b$ equal to zero in equation (38). For a given value of the rarefaction parameter (or, alternately, mean free path), the effect of increasing heat flux ratio is to reduce the temperature difference $(t_{w,1} - t_b)_d$. The accommodation coefficient also has an important effect on the temperature difference. Smaller values of a give rise to a higher contact resistance between gas and wall and thereby increase the temperature difference $(t_{w,1} - t_b)_d$. The effects of gas rarefaction and accommodation coefficient on the temperature difference at the lower wall $(t_{w,2} - t_b)_d$ are similar to those exhibited for the upper wall temperature difference. For a given mean free path, however, increasing the heat flux ratio increases the temperature difference.

The ratios of local to fully developed temperature differences at any location in the channel are found from equations (35) to (39) as

$$\frac{t_{w,1} - t_b}{(t_{w,1} - t_b)_d} =$$

$$\frac{G\left(1, \frac{u_s}{\bar{u}}\right) + 4\frac{q_1}{q_1 + q_2}\frac{\xi_t}{2b} + \sum_{n=1}^{\infty} a_n Y_n(1)\exp\left(\frac{-4\lambda_n \frac{x}{2b}}{RePr}\right) + \frac{q_1 - q_2}{q_1 + q_2}\left[1 + \sum_{n=0}^{\infty} b_n Z_n(1)\exp\left(\frac{-4\gamma_n \frac{x}{2b}}{RePr}\right)\right]}{G\left(1, \frac{u_s}{\bar{u}}\right) + 4\frac{q_1}{q_1 + q_2}\frac{\xi_t}{2b} + \frac{q_1 - q_2}{q_1 + q_2}} \tag{40}$$

$$\frac{t_{w,2} - t_b}{(t_{w,2} - t_b)_d} =$$

$$\frac{G\left(1, \frac{u_s}{\bar{u}}\right) + 4\frac{q_2}{q_1 + q_2}\frac{\xi_t}{2b} + \sum_{n=1}^{\infty} a_n Y_n(1)\exp\left(\frac{-4\lambda_n \frac{x}{2b}}{RePr}\right) - \frac{q_1 - q_2}{q_1 + q_2}\left[1 + \sum_{n=0}^{\infty} b_n Z_n(1)\exp\left(\frac{-4\gamma_n \frac{x}{2b}}{RePr}\right)\right]}{G\left(1, \frac{u_s}{\bar{u}}\right) + 4\frac{q_2}{q_1 + q_2}\frac{\xi_t}{2b} - \frac{q_1 - q_2}{q_1 + q_2}} \tag{41}$$

where

$$G\left(1, \frac{u_s}{\bar{u}}\right) = \frac{17}{35} - \frac{6}{35}\frac{u_s}{\bar{u}} + \frac{2}{105}\left(\frac{u_s}{\bar{u}}\right)^2 \tag{42}$$

Equations (40) and (41) can be evaluated when numerical values of λ_n, γ_n, $Y_n(1)$, $Z_n(1)$, a_n, and b_n have been obtained for given values of $u_s/\bar{u}$.

It is of interest to examine the wall to bulk temperature differences at the entrance of the heated section. This is done by setting $x = 0$ in equations (40) and (41) to give the results

$$\frac{(t_{w,1} - t_b)_0}{(t_{w,1} - t_b)_d} =$$

$$\frac{G\left(1, \frac{u_s}{\bar{u}}\right) + 4\frac{q_1}{q_1 + q_2}\frac{\xi_t}{2b} + \sum_{n=1}^{\infty} a_n Y_n(1) + \frac{q_1 - q_2}{q_1 + q_2}\left[1 + \sum_{n=0}^{\infty} b_n Z_n(1)\right]}{G\left(1, \frac{u_s}{\bar{u}}\right) + 4\frac{q_1}{q_1 + q_2}\frac{\xi_t}{2b} + \frac{q_1 - q_2}{q_1 + q_2}} \tag{43}$$

$$\frac{(t_{w,2} - t_b)_0}{(t_{w,2} - t_b)_d} =$$

$$\frac{G\left(1, \frac{u_s}{\bar{u}}\right) + 4\frac{q_2}{q_1 + q_2}\frac{\xi_t}{2b} + \sum_{n=1}^{\infty} a_n Y_n(1) - \frac{q_1 - q_2}{q_1 + q_2}\left[1 + \sum_{n=0}^{\infty} b_n Z_n(1)\right]}{G\left(1, \frac{u_s}{\bar{u}}\right) + 4\frac{q_2}{q_1 + q_2}\frac{\xi_t}{2b} - \frac{q_1 - q_2}{q_1 + q_2}} \tag{44}$$

According to equations (25) and (26), however, when $\eta = 1$,

$$\sum_{n=1}^{\infty} a_n Y_n(1) = -G\left(1, \frac{u_s}{\bar{u}}\right)$$

and

$$\sum_{n=0}^{\infty} b_n Z_n(1) = -1$$

Then equations (43) and (44) reduce to the simpler expressions

$$\frac{(t_{w,1} - t_b)_0}{(t_{w,1} - t_b)_d} = \frac{\dfrac{4q_1 \frac{\xi_t}{2b}}{q_1 + q_2}}{G\left(1, \frac{u_s}{\bar{u}}\right) + \dfrac{4q_1 \frac{\xi_t}{2b}}{q_1 + q_2} + \dfrac{q_1 - q_2}{q_1 + q_2}} \tag{45}$$

$$\frac{(t_{w,2} - t_b)_0}{(t_{w,2} - t_b)_d} = \frac{\dfrac{4q_2 \frac{\xi_t}{2b}}{q_1 + q_2}}{G\left(1, \frac{u_s}{\bar{u}}\right) + \dfrac{4q_2 \frac{\xi_t}{2b}}{q_1 + q_2} - \dfrac{q_1 - q_2}{q_1 + q_2}} \tag{46}$$

In the absence of a temperature jump, the wall to bulk temperature difference is zero at the entrance for either plate. With a temperature jump, however, the entrance temperature difference can have a nonzero value. Equations (45) and (46) have been plotted in figure 3 as functions of the parameters $u_s/\bar{u}$,

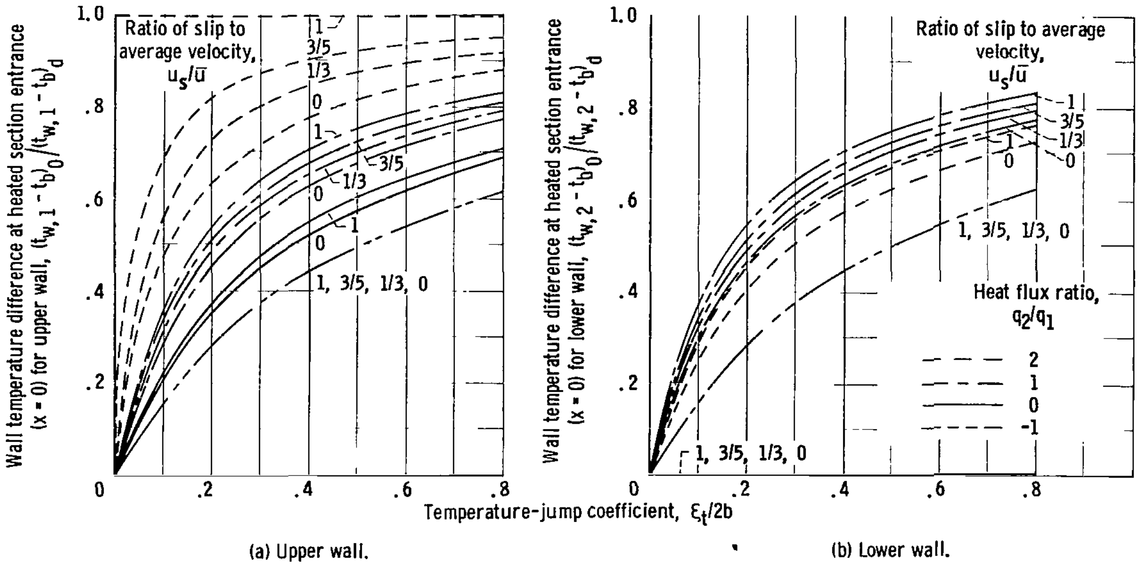

Figure 3. - Wall temperature ratio at heated section entrance.

$\xi_t/2b$, and q_2/q_1. The entrance temperature difference at the upper wall increases with increasing values of $\xi_t/2b$ for all values of q_2/q_1 shown. For a given value of $\xi_t/2b$, increasing the heat flux ratio increases the entrance temperature difference. The ratio of slip to average velocity has only a small influence on the quantity $(t_{w,1} - t_b)_0/(t_{w,1} - t_b)_d$ for small values of the heat flux ratio, while for $q_2/q_1 = 2$ the influence of the slip velocity is more pronounced.

The entrance temperature difference at the lower wall likewise increases with increasing values of $\xi_t/2b$ for all values of q_2/q_1 considered. For a fixed value of $\xi_t/2b$, however, symmetrical heating, which corresponds to $q_2/q_1 = 1$, has the most pronounced effect on the temperature difference $(t_{w,2} - t_b)_0/(t_{w,2} - t_b)_d$. It is interesting to note that, when the heat addition at the upper wall is equal to the heat extraction at the lower wall, the ratio of slip to average velocity has no effect on the entrance temperature difference at either wall.

Transverse Distribution Functions $Y(\eta)$, $Z(\eta)$

Attention is now directed to the Sturm-Liouville eigenvalue problems (eqs. (20) and (22)). The even function $Y(\eta)$ is the solution of equation (20) and the normalization convention $Y(0) = 1$. Asymptotic expressions for the even eigenvalues λ_n and constants a_n and $Y_n(1)$ are given in reference 5 and the results are presented here to make the analysis more complete:

$$\beta_n \tan \beta_n = \frac{\sqrt{4\theta} + (1 + 4\theta)\sin^{-1} \frac{1}{\sqrt{1 + 4\theta}}}{4(4\theta)^{3/2}} \equiv C \tag{47}$$

$$A_n \equiv a_n Y_n(1) = \frac{-16\theta}{C + 1 + \frac{\lambda_n^2}{C}} \tag{48}$$

where

$$\beta_n \equiv \sqrt{\lambda_n}\, I_1 \tag{49}$$

$$I_1 \equiv \int_0^1 \sqrt{f(\eta)}\, d\eta = \frac{\sqrt{\frac{3}{8}}\left[\sqrt{4\theta} + (1 + 4\theta)\sin^{-1} \frac{1}{\sqrt{1 + 4\theta}}\right]}{\sqrt{1 + 6\theta}} \tag{50}$$

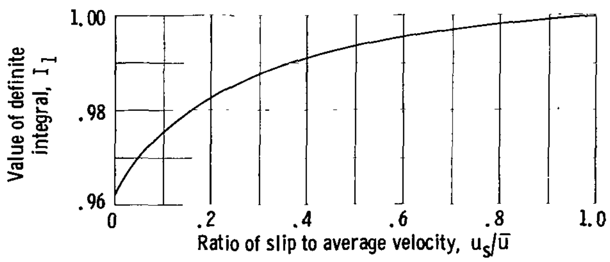

Figure 4. - Value of definite integral for any value of slip to average velocity ratio.

The first five roots of equation (47) are given in reference 7 for a number of values of C. The values of I_1 for any given slip velocity $u_s/\bar{u}$ are shown in figure 4.

The even eigenvalues and constants for the limiting case of slug flow ($u_s/\bar{u} \rightarrow 1$) between parallel plates are given in reference 5 as

$$\sqrt{\lambda_n} = n\pi \qquad n = 1, 2, \ldots \tag{51}$$

$$A_n = -\frac{2}{\lambda_n} \tag{52}$$

The odd eigenvalues γ_n and constants b_n and $Z_n(1)$ are determined from the solution of equation (22) and the condition $Z(0) = 0$. By applying the methods presented in reference 5 to determine the asymptotic expressions for symmetrical heating, it is readily found that the asymptotic solution of equation (22) satisfying the condition $Z(0) = 0$ is

$$Z(\eta) = F(1 + 4\theta)^{1/4}(1 - \eta^2 + 4\theta)^{-1/4} \sin (\sqrt{\gamma}\, J) \tag{53}$$

where F is an arbitrary constant, and

$$J \equiv \int_0^{\eta} \sqrt{f(\eta)}\, d\eta = \frac{\sqrt{\frac{3}{8}}\left[\eta\sqrt{1 - \eta^2 + 4\theta} + (1 + 4\theta)\sin^{-1}\frac{\eta}{\sqrt{1 + 4\theta}}\right]}{\sqrt{1 + 6\theta}} \tag{54}$$

From the condition $dZ/d\eta = 0$ at $\eta = 1$, the eigenvalues γ_n are obtained as the roots of the characteristic equation

$$\delta_n \cot \delta_n = - \frac{\sqrt{4\theta} + (1 + 4\theta)\sin^{-1}\frac{1}{\sqrt{1 + 4\theta}}}{4(4\theta)^{3/2}} = -C \tag{55}$$

where

$$\delta_n \equiv \sqrt{\gamma_n}\, J_1 \tag{56a}$$

$$J_1 \equiv \int_0^1 \sqrt{f(\eta)}\, d\eta = I_1 \tag{56b}$$

The first six roots of equation (55) are given in reference 7 for a number of values of C.

The constants $Z_n(1)$ are obtained by setting $\gamma = \gamma_n$ and $\eta = 1$ in equation (53), which results in

$$Z_n(1) = F\left(\frac{1 + 4\theta}{4\theta}\right)^{1/4} \sin \delta_n \tag{57}$$

The series coefficients b_n are found from equations (30) and (53) as

$$b_n = - \frac{4(4\theta)^{5/4}}{F(1 + 4\theta)^{1/4}\left(C + 1 + \frac{\gamma_n^2}{C}\right)\sin \delta_n} \tag{58}$$

It is convenient to introduce a new constant B_n, defined as the product of b_n and $Z_n(1)$

$$B_n \equiv b_n Z_n(1) = \frac{-16\theta}{C + 1 + \frac{\gamma_n^2}{C}} \tag{59}$$

A noteworthy feature of equation (59) is that the coefficients B_n are independent of the arbitrary constant F.

For the limiting case of slug flow ($f(\eta) \to 1$) between parallel plates, the odd eigenvalues and constants are obtained from the solution of the equation

$$\left.\begin{aligned} &\frac{d^2Z_n}{d\eta^2} + \gamma_n Z_n = 0 \\ &Z_n(0) = 0, \ \frac{dZ_n}{d\eta} = 0 \qquad \text{at} \quad \eta = -1 \quad \text{and} \quad \eta = +1 \end{aligned}\right\} \tag{60}$$

The eigenvalues are given by $\sqrt{\gamma_n} = (2n + 1)\pi/2$. For $f(\eta) \to 1$ the eigenfunctions evaluated at the wall are given as $Z_n(1) = (-1)^n F$, while the coefficients approach $b_n|_{f(\eta)\to 1} = (-1)^{n+1} 2/F\gamma_n$. Then the coefficients B_n are given as $B_n = -2/\gamma_n$.

The first four values of $\sqrt{\lambda_n}$ together with the corresponding values of A_n are listed in table I for several values of the ratio of slip to average

TABLE I. - EVEN EIGENVALUES AND COEFFICIENTS FOR LAMINAR SLIP FLOW

IN PARALLEL-PLATE CHANNEL WITH UNSYMMETRICAL WALL HEAT FLUX

	Ratio of slip to average velocity, $u_s/\bar{u}$					
	0	1/3		3/5		1
		Analytical solution	Numerical solution	Analytical solution	Numerical solution	
	Eigenvalue					
$\sqrt{\lambda_1}$	3.540	3.78	3.33	3.35	3.23	3.141
$\sqrt{\lambda_2}$	6.800	6.72	6.49	6.41	6.36	6.282
$\sqrt{\lambda_3}$	10.05	9.78	9.65	9.54	9.50	9.423
$\sqrt{\lambda_4}$	13.30	12.90	12.82	12.69	12.65	12.56
	Coefficient					
A_1	-0.2090	-0.1479	-0.2331	-0.2110	-0.2264	-0.2030
A_2	-.0703	-.0642	-.0701	-.0613	-.0618	-.0508
A_3	-.0367	-.0332	-.0336	-.0281	-.0282	-.0226
A_4	-.0230	-.0198	-.0197	-.0165	-.0161	-.0127

velocity. The first four values of $\sqrt{\gamma_n}$ together with the corresponding values of B_n are listed in table II for the same values of $u_s/\bar{u}$. The results for continuum flow were obtained from reference 4. To check the level of accuracy for the slip-flow values, equations (20) and (22) were solved numeri-

TABLE II. - ODD EIGENVALUES AND COEFFICIENTS FOR LAMINAR SLIP FLOW

IN PARALLEL-PLATE CHANNEL WITH UNSYMMETRICAL WALL HEAT FLUX

	Ratio of slip to average velocity, $u_s/\bar{u}$					
	0	1/3		3/5		1
		Analytical solution	Numerical solution	Analytical solution	Numerical solution	
	Eigenvalue					
$\sqrt{\gamma_1}$	1.845	2.411	1.748	1.915	1.673	1.571
$\sqrt{\gamma_2}$	5.125	5.225	4.906	4.875	4.790	4.712
$\sqrt{\gamma_3}$	8.405	8.250	8.066	7.975	7.927	7.854
$\sqrt{\gamma_4}$	11.68	11.35	11.23	11.11	11.07	11.00
	Coefficient					
B_1	-0.6641	-0.2309	-0.7286	-0.5495	-0.7678	-0.8100
B_2	-.1157	-.0983	-.1163	-.1049	-.1068	-.0902
B_3	-.0504	-.0513	-.0469	-.0402	-.0402	-.0324
B_4	-.0289	-.0254	-.0253	-.0209	-.0208	-.0166

cally by means of the Runge-Kutta method on an IBM 7094 digital computer. Reference 5 has presented numerical values for the even quantities λ_n and A_n, and the results are given in table I. Equation (22) was solved numerically in the course of the present investigation. The forward integration was started by using the condition $Z_n(0) = 0$ and by arbitrarily letting $(dZ_n/d\eta)_{\eta=0} = 1$. The eigenvalues were found by trial and error until the zero-derivative boundary condition was satisfied at $\eta = 1$. The first four odd eigenvalues γ_n and constants B_n are given in table II. The even and odd quantities as computed from the previously presented analytical expressions are in close agreement with the values obtained by means of the Runge-Kutta method, especially for $n \geq 2$. In view of the very good level of agreement that is demonstrated, it is concluded that the formulas for the even and odd quantities are suitable for $n \geq 2$.

Wall Temperature Distributions

With the numerical information in tables I and II the dimensionless wall temperature variation along the upper wall as given by equation (40) and along the lower wall as given by equation (41) are plotted in figures 5 to 12 for various values of $u_s/\bar{u}$ and $\xi_t/2b$ and for a few values of q_2/q_1.

Inspection of figures 5 to 12 reveals several interesting trends. For the

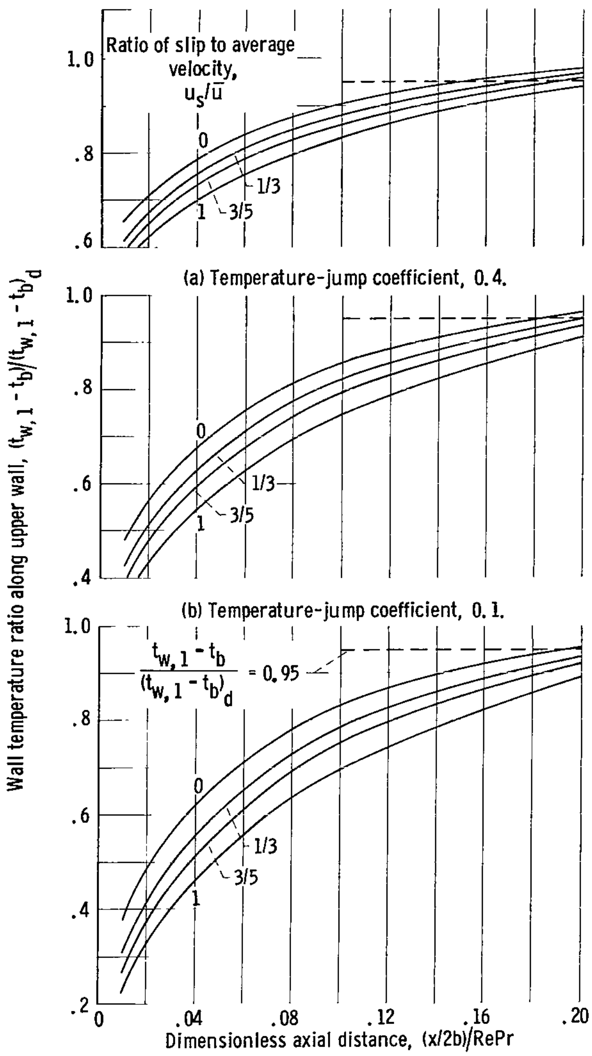

(a) Temperature-jump coefficient, 0.4.

(b) Temperature-jump coefficient, 0.1.

(c) Temperature-jump coefficient, 0.

Figure 5. - Wall temperature ratio along upper wall in thermal entrance region. Heat flux ratio, -1.

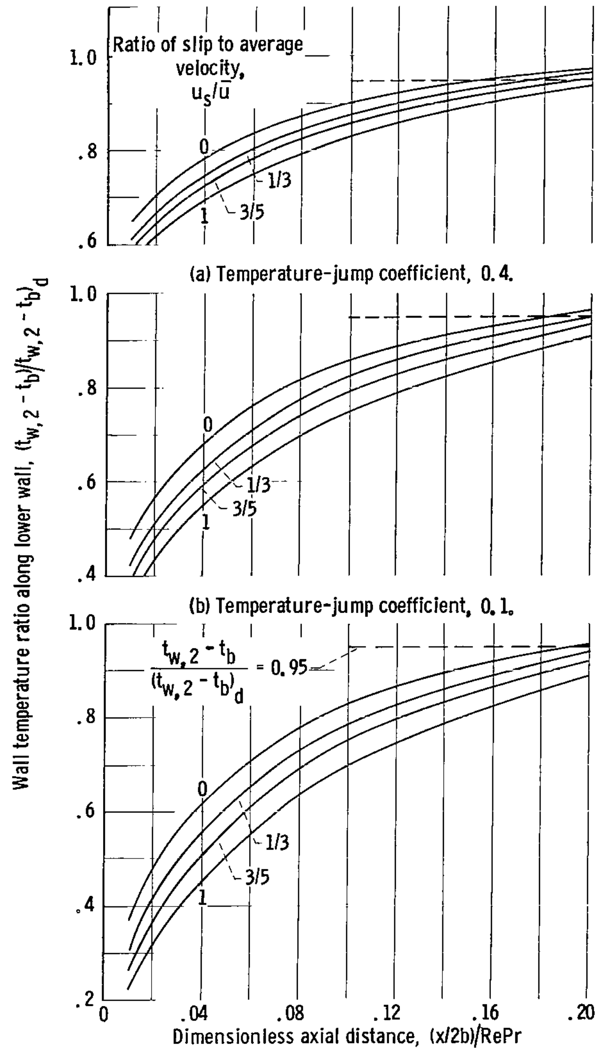

(a) Temperature-jump coefficient, 0.4.

(b) Temperature-jump coefficient, 0.1.

(c) Temperature-jump coefficient, 0.

Figure 6. - Wall temperature ratio along lower wall in thermal entrance region. Heat flux ratio, -1.

various wall heating situations represented, increasing the slip velocity decreases the difference between bulk and wall temperature at a given axial position in the thermal entrance region, while the temperature jump increases the difference. Thus the slip velocity has the effect of retarding $t_w - t_b$ in its approach to the fully developed value, while the temperature jump has the opposite effect. It is noteworthy that the wall temperature ratios $(t_{w,1} - t_b)/(t_{w,1} - t_b)_d$ and $(t_{w,2} - t_b)/(t_{w,2} - t_b)_d$ are identical for heat flux ratios of -1 and 1.

A thermal entrance length can be arbitrarily defined as the length required for $t_w - t_b$ to be within 5 percent of the fully developed value. A horizontal dashed line corresponding to an ordinate of 0.95 is shown in figures

5 to 10 and 12. The increase in thermal entrance length with increasing slip is apparent. For a given ratio of slip to average velocity, increasing the temperature jump decreases the thermal entrance length. It should be noted that the length required to approach fully developed conditions, for given velocity-slip and temperature-jump values, is greater for unsymmetrical heating than for symmetrical wall heat flux.

It is of interest to present the wall to bulk temperature differences in the thermal entrance region in terms

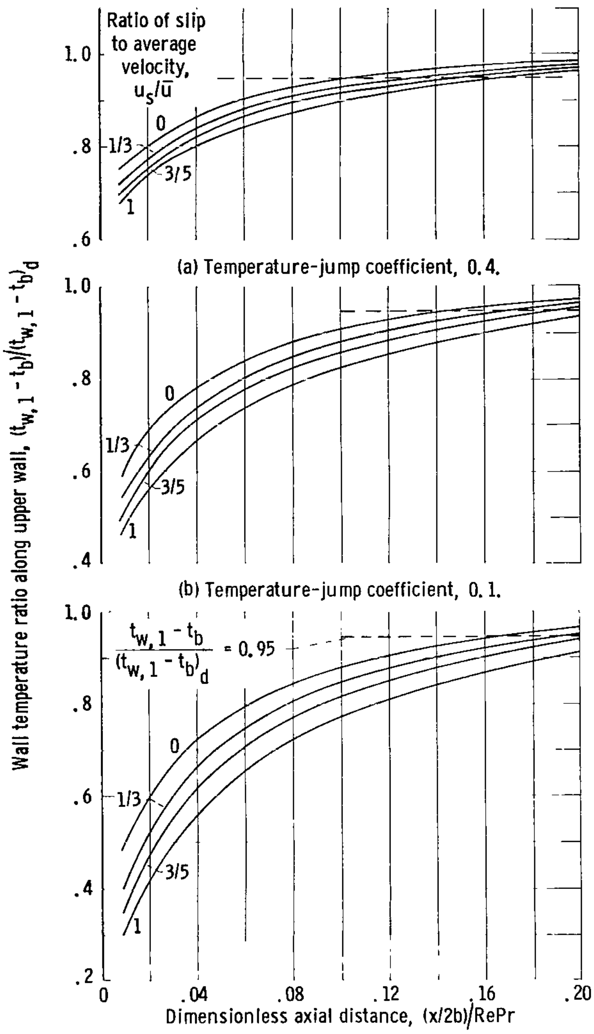

(a) Temperature-jump coefficient, 0.4.

(b) Temperature-jump coefficient, 0.1.

(c) Temperature-jump coefficient, 0.

Figure 7. - Wall temperature ratio along upper wall in thermal entrance region. Heat flux ratio, 0.

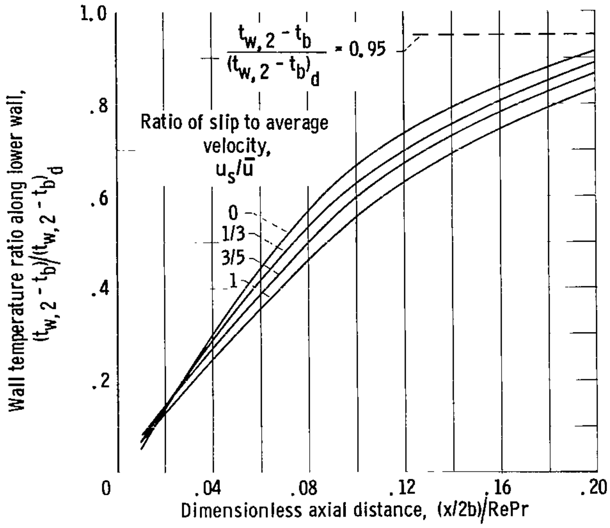

Figure 8. - Wall temperature ratio along lower wall in thermal entrance region. Heat flux ratio, 0.

of the rarefaction parameter $\mu\sqrt{R_g t}/2pb$. This has been done in figures 13 to 16 for several values of the heat flux ratio. The abscissas cover values of $\mu\sqrt{R_g t}/2pb$ ranging from 0 to 0.20, even though this latter value may perhaps be outside the slip regime, since at lower densities, in the beginning of the transition regime, prior findings suggest that slip-flow solutions may remain fairly good (ref. 6). For all values of the heat flux ratio except $q_2/q_1 = 0$, increasing the gas rarefaction shortens the thermal entrance length at either wall. The increase in temperature jump with a decrease in accommodation coefficient also has an important effect on the thermal entrance length. For the heat flux ratio $q_2/q_1 = 0$, increasing the rarefaction decreases the entrance length at the heated upper wall (fig. 14(a)), while it increases the entrance length at the insulated lower wall (fig. 14(b)). For a given mean free path, the length required for the wall temperature ratio to approach unity is least for the channel with symmetrical wall heat flux (fig. 15), as noted earlier.

OTHER RAREFACTION EFFECTS

Several other, less frequently considered rarefaction effects have been cited in the literature and, for the sake of completeness, modification of the heat-transfer results will be made or discussed to account for these slip effects.

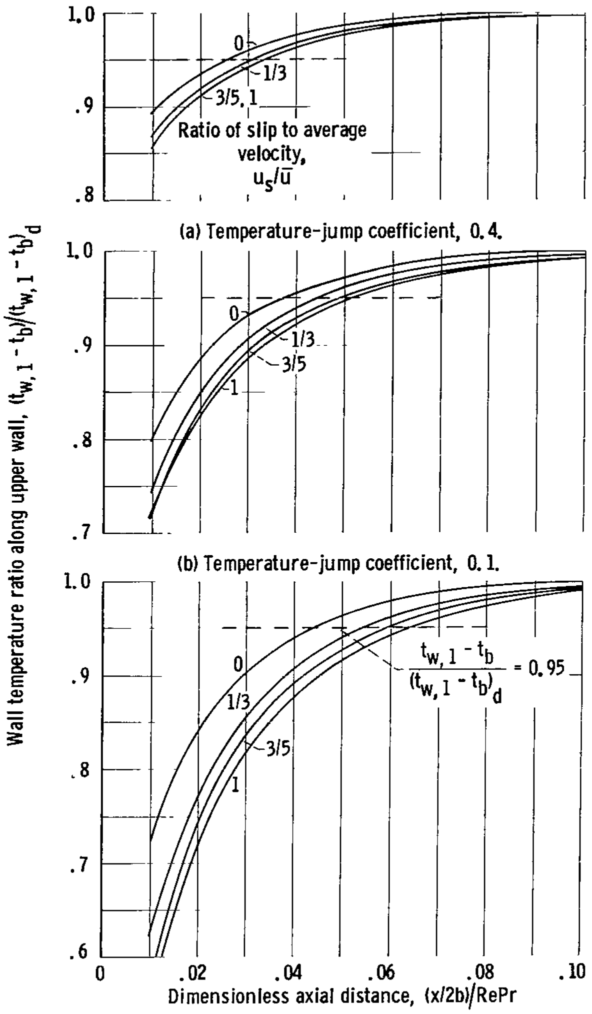

(a) Temperature-jump coefficient, 0.4.

(b) Temperature-jump coefficient, 0.1.

(c) Temperature-jump coefficient, 0.

Figure 9. - Wall temperature ratio along upper wall in thermal entrance region. Heat flux ratio, 1.

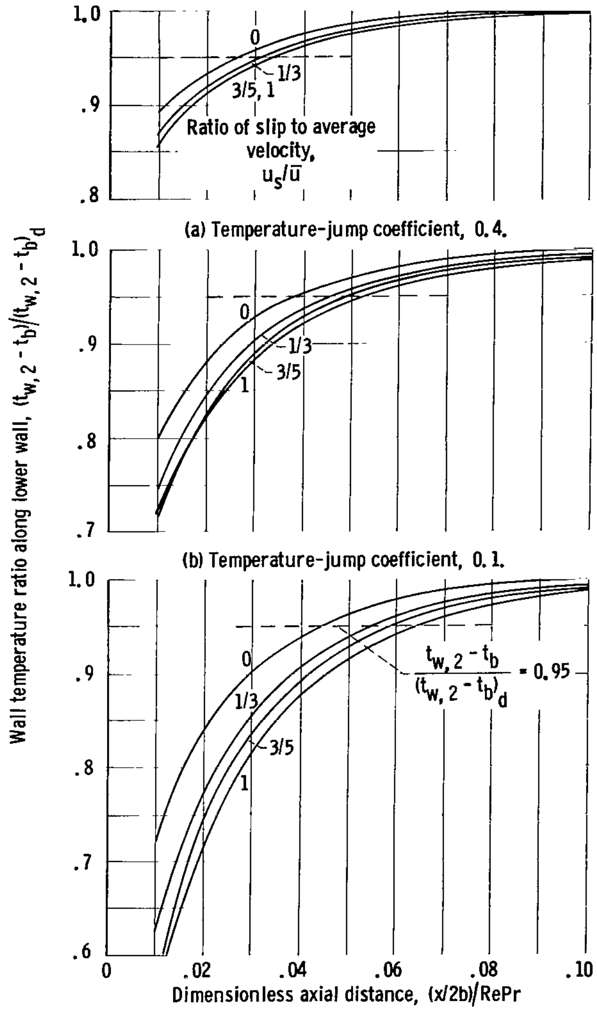

(a) Temperature-jump coefficient, 0.4.

(b) Temperature-jump coefficient, 0.1.

(c) Temperature-jump coefficient, 0.

Figure 10. - Wall temperature ratio along lower wall in thermal entrance region. Heat flux ratio, 1.

Wall Shear Work

It is proposed in reference 8 that when there is a slip flow an energy balance at the wall must include the shear work done by the slipping gas. Denoting, as before, the heat transfer from the upper and lower walls by q_1 and q_2, respectively, the proposal is equivalent to writing the temperature derivative at the walls in the fully developed region as

$$\kappa\left(\frac{\partial t}{\partial y}\right)_{y=b} = q_1 + q^* \tag{61a}$$

$$\kappa\left(\frac{\partial t}{\partial y}\right)_{y=-b} = -(q_2 + q^*) \tag{61b}$$

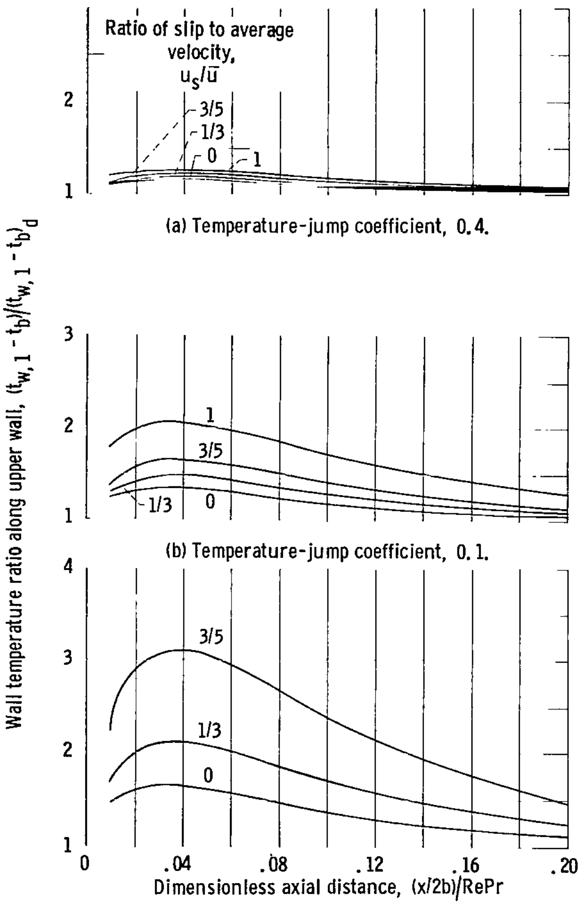

(c) Temperature-jump coefficient, 0.

Figure 11. - Wall temperature ratio along upper wall in thermal entrance region. Heat flux ratio, 2.

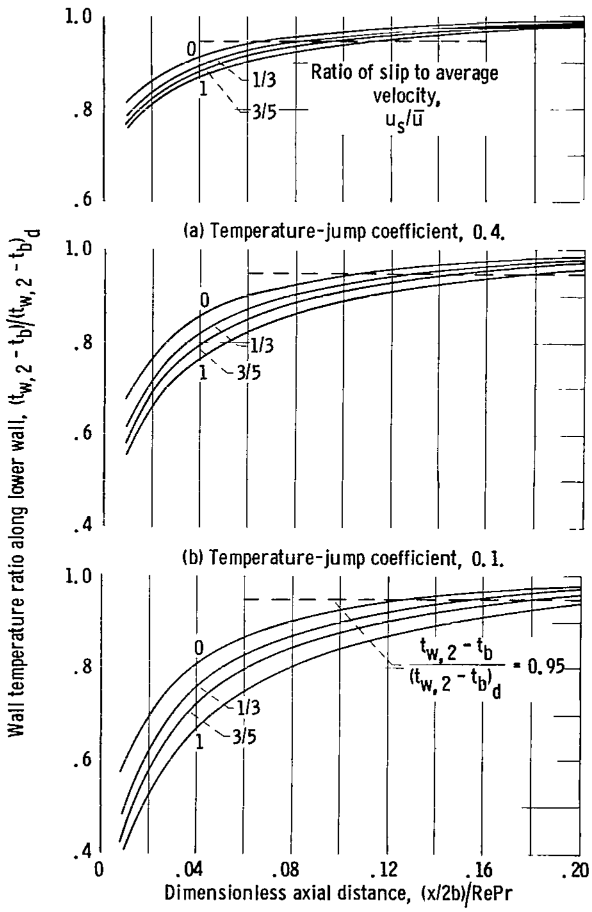

(c) Temperature-jump coefficient, 0.

Figure 12. - Wall temperature ratio along lower wall in thermal entrance region. Heat flux ratio, 2.

where q^* is an equivalent heat flux defined as

$$q^* = \frac{\mu u_s^2}{\xi_u} \tag{62}$$

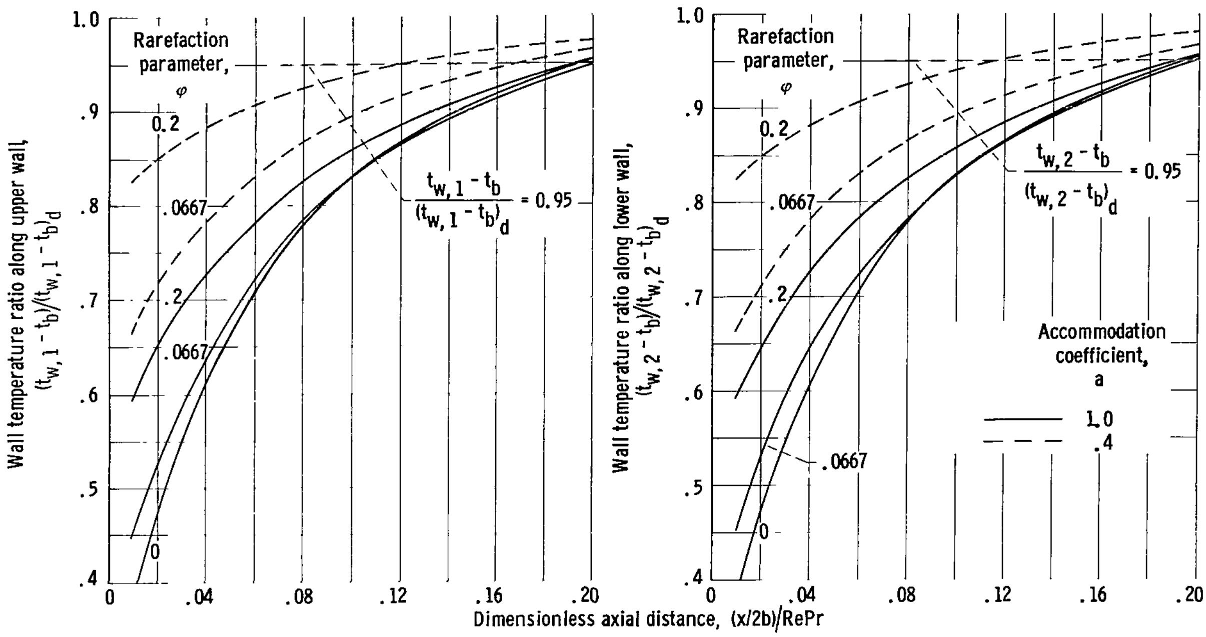

(a) Upper wall.

(b) Lower wall.

Figure 13. - Wall temperature ratio in thermal entrance region. Specular reflection coefficient, 1; specific heat ratio, 1.4; Prandtl number, 0.73; heat flux ratio, -1.

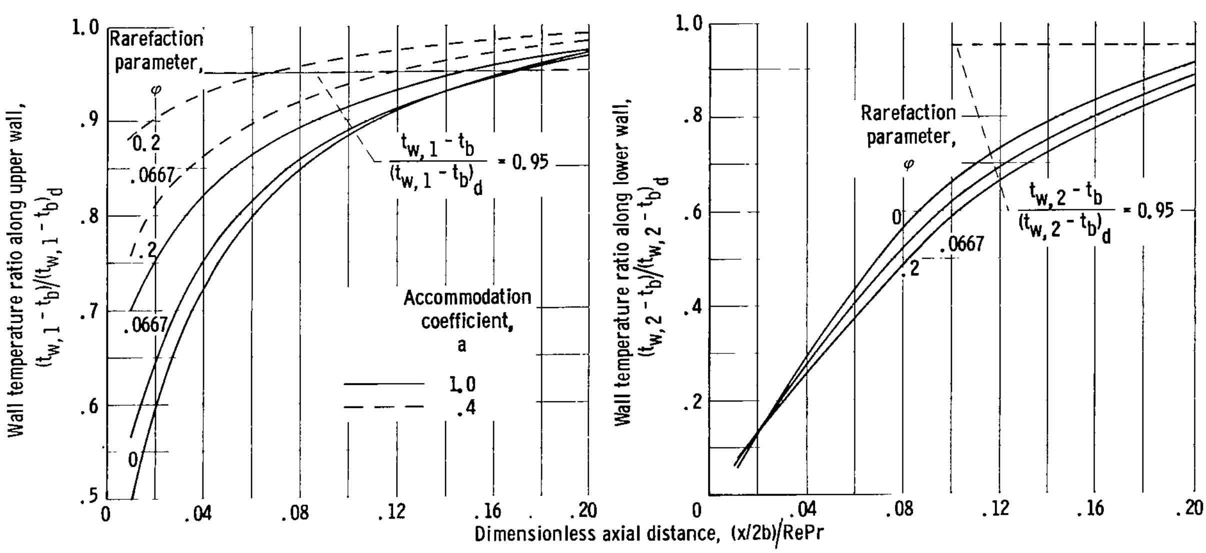

(a) Upper wall.

(b) Lower wall.

Figure 14. - Wall temperature ratio in thermal entrance region. Specular reflection coefficient, 1; specific heat ratio, 1.4; Prandtl number, 0.73; heat flux ratio, 0.

Then if everywhere that q_1 and q_2 formerly appeared $q_1 + q^*$ and $q_2 + q^*$, respectively, are now written, the prior analysis continues to be applicable. For an "adiabatic" lower plate ($q_2 = 0$), the temperature derivative at the wall is now given by $(\partial t/\partial y)_{y=-b} = -q^*/\kappa$.

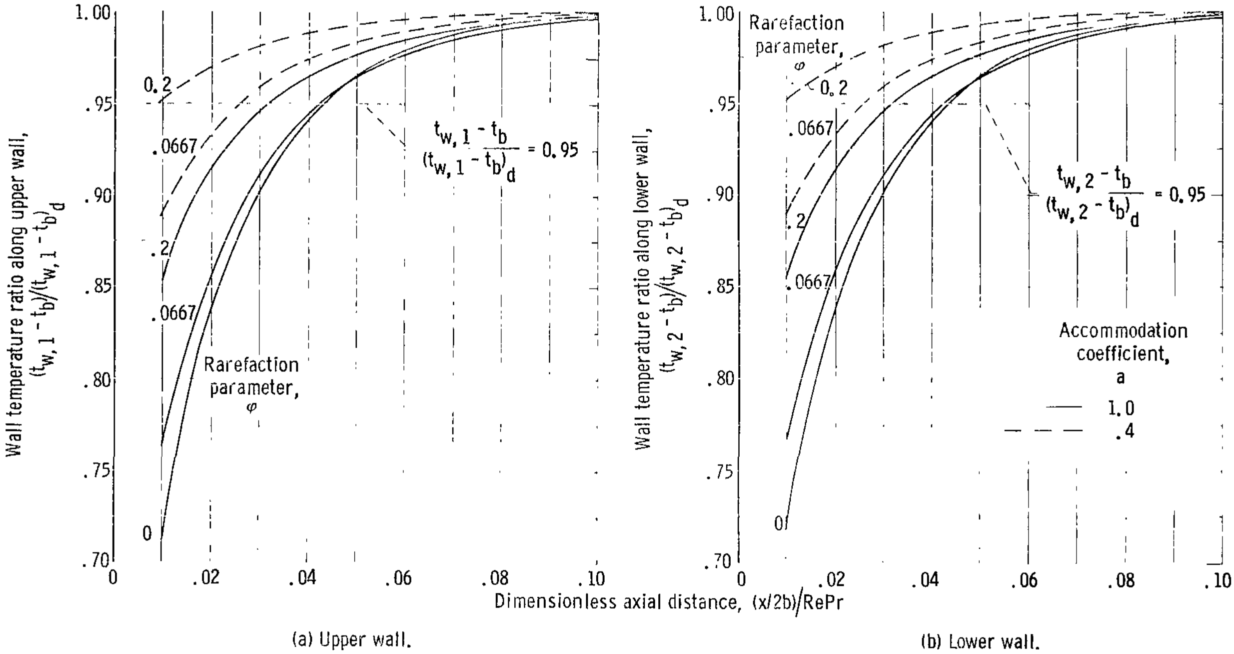

Figure 15. - Wall temperature ratio in thermal entrance region. Specular reflection coefficient, 1; specific heat ratio, 1.4; Prandtl number, 0.73; heat flux ratio, 1.

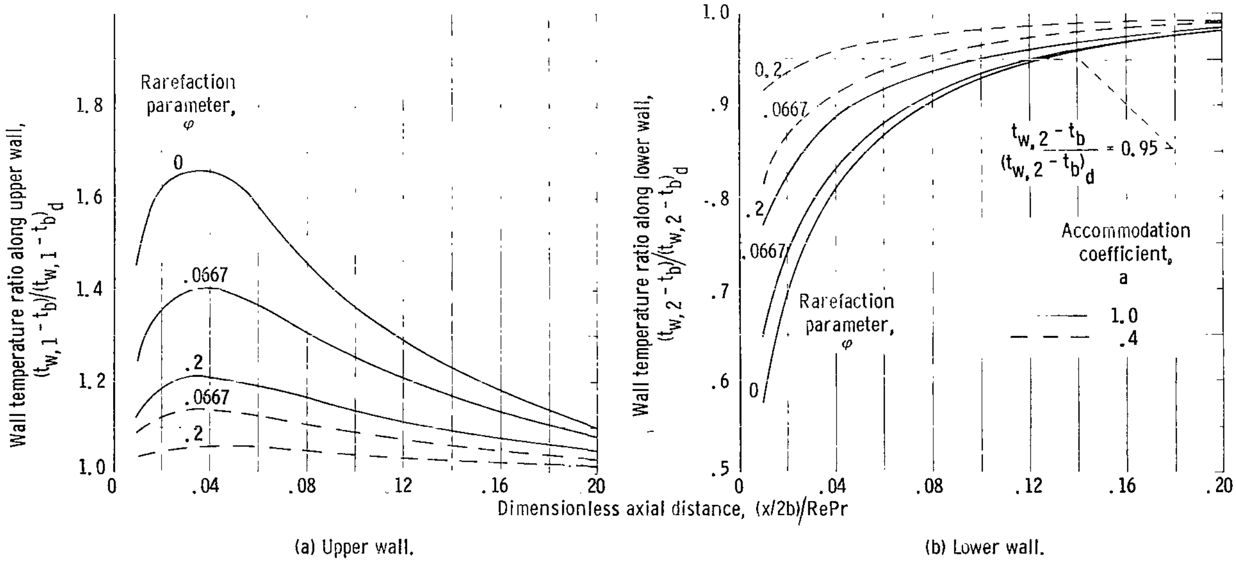

Figure 16. - Wall temperature ratio in thermal entrance region. Specular reflection coefficient, 1; specific heat ratio, 1.4; Prandtl number, 0.73; heat flux ratio, 2.

Modified Temperature Jump

The temperature jump derived for a stationary gas should be modified for a moving gas (ref. 9). The proposal is tantamount to altering equations (32a) and (32b) to read

$$t_{g,1} - t_{w,1}^{*} = -2\,\frac{\xi_t}{2b}\left(\frac{\partial t}{\partial \eta}\right)_{\eta=1} \tag{63a}$$

$$t_{g,2} - t_{w,2}^{*} = 2\,\frac{\xi_t}{2b}\left(\frac{\partial t}{\partial \eta}\right)_{\eta=-1} \tag{63b}$$

respectively, where

$$t_w^{*} = t_w + \left(\frac{4\sigma}{\sigma + 1} + \frac{1 - a}{a}\,\frac{g}{2 - g}\right)\frac{u_s^2}{c_p} \tag{64}$$

Hence if $t_{w,1}$ and $t_{w,2}$ are replaced at all places by $t_{w,1}^{*}$ and $t_{w,2}^{*}$, respectively, the foregoing developments continue to apply.

Thermal Creep

When a gas adjacent to a surface encounters a temperature gradient along the surface, there will be an additional velocity (thermal creep) induced in the direction of increasing temperature (ref. 10) and the slip velocity is altered from that given in reference 5 to

$$u_s = \pm\xi_u\left(\frac{\partial u}{\partial y}\right)_{y=\mp b} + \frac{3}{4}\,\frac{\mu R_g}{p}\left(\frac{\partial t}{\partial x}\right)_{y=\mp b} \tag{65}$$

The analysis in the main body of the investigation has not included the thermal creep velocity. As a consequence, the velocity field could be determined independently of the temperature and treated as fully developed. If thermal creep is not negligible, the temperature and velocity fields are mutually interdependent, and the momentum and energy equation system for the gas presents an extremely complicated mathematical problem. In the fully developed heat-transfer region, of course, $\partial t/\partial x$ is a constant and the thermal creep can be included in equation (65) without difficulty. In the thermal entrance region, however, $\partial t/\partial x$ varies with x.

The present solutions without the inclusion of thermal creep are still very useful, since they represent the zeroth-order solutions. The range of validity of the present solutions must be established primarily by comparison with experimental data. Within the knowledge of the author, there are no heat-transfer measurements for low-density flows in conduits available with which to compare the results predicted herein. A more general analysis that would take into account thermal creep is also well in order. In any event, the present analytical solutions should prove useful to the design engineer by offering a method that allows, in the absence of thermal creep, a rapid determination of the eigenvalues and the coefficients of the series expansions with high accuracy. This in turn allows for a rapid determination of the heat transfer in design calculations. Finally, the analysis exhibits general effects of slight gas rarefaction and wall heat fluxes on forced-convection heat transfer in channels.

CONCLUDING REMARKS

Solutions have been obtained for laminar, forced-convection heat transfer to a slightly rarefied gas flowing between parallel plates with constant (but unequal) heat fluxes at the plates. The wall temperatures in both the entrance and fully developed regions can be obtained as functions of the velocity and temperature jumps at the wall, or as functions of the mean free path, for various wall heat flux ratios. Several cases of general interest are considered, and the solutions are given in graphical form to illustrate the effects of slight rarefaction and wall heat flux ratio on heat transfer to a flowing gas.

Lewis Research Center
National Aeronautics and Space Administration
Cleveland, Ohio, June 9, 1964

APPENDIX - SYMBOLS

A_n	coefficient defined in eq. (48)
a	accommodation coefficient
a_n	coefficient in even series expansion
B_n	coefficient defined in eq. (59)
b	half distance between plates
b_n	coefficient in odd series expansion
C	constant defined in eq. (47)
c_p	specific heat of gas
F	arbitrary constant
$f(\eta)$	dimensionless velocity, $u(\eta)/\overline{u}$
$G(\eta,u_s/\overline{u})$	function defined by eq. (25)
g	specular reflection coefficient
$H(\eta)$	transverse temperature distribution in fully developed region
I_1	definite integral defined in eq. (50)
J	indefinite integral defined in eq. (54)
J_1	definite integral defined in eq. (56b), equal to I_1
l	mean free path
Pr	Prandtl number, $\mu c_p/\kappa$
p	gas pressure
q	rate of heat transfer per unit area from wall to gas
q^*	shear work at wall
Re	Reynolds number, $2\rho\overline{u}b/\mu$
R_g	gas constant
t	gas temperature
t_g	temperature of gas adjacent to wall

u gas velocity

x axial coordinate

Y even transverse distribution function

Y_n eigenfunctions of eq. (20)

y transverse coordinate

Z odd transverse distribution function

Z_n eigenfunctions of eq. (22)

α thermal diffusivity, $\kappa/\rho c_p$

β_n $-\sqrt{\lambda_n}\ I_1$

γ_n eigenvalues of eq. (22)

δ_n $-\sqrt{\gamma_n}\ J_1$

ζ dimensionless axial distance, $4(x/2b)/RePr$

η dimensionless transverse coordinate, y/b

θ dimensionless velocity slip coefficient, $\xi_u/2b$

κ gas thermal conductivity

λ_n eigenvalues of eq. (20)

μ gas viscosity

ξ_t temperature-jump coefficient

ξ_u velocity-slip coefficient

ρ gas density

σ ratio of specific heats

Φ function defined in eq. (16)

φ rarefaction parameter, $\mu\sqrt{R_g t}/2pb$

Ω function defined in eq. (16)

Subscripts:

b gas bulk condition

d fully developed region

e entrance region

s slip

w wall condition

0 entrance, $x = 0$

1 upper wall, $y = b$

2 lower wall, $y = -b$

Superscript:

- average

REFERENCES

1. Yih, C. S., and Cermak, Jack E.: Laminar Heat Convection in Pipes and Ducts. Rep. 5, Civil Eng. Dept., Colorado College of Agricultural and Mech. Arts, Sept. 1951.

2. Schenk, J., and Beckers, H. L.: Heat Transfer in Laminar Flow Between Parallel Plates. Appl. Sci. Res., sec. A, vol. 4, no. 1, 1953-54, pp. 405-413.

3. Cess, R. D., and Shaffer, E. C.: Summary of Laminar Heat Transfer Between Parallel Plates with Unsymmetrical Wall Temperatures. Jour. Aero/Space Sci., vol. 26, no. 8, Aug. 1959, p. 538.

4. Cess, R. D., and Shaffer, E. C.: Laminar Heat Transfer Between Parallel Plates With an Unsymmetrically Prescribed Heat Flux at the Walls. Appl. Sci. Res., sec. A, vol. 9, 1959, pp. 64-70.

5. Inman, Robert M.: Heat Transfer to Laminar Slip Flow of a Rarefied Gas in a Parallel-Plate Channel or a Round Tube with Uniform Wall Heat Flux. NASA TN D-2393, 1964.

6. Schaaf, S. A., and Chambre, P. L.: Flow of Rarefied Gases. Princeton Univ. Press, 1961, p. 34.

7. Carslaw, H. S., and Jaeger, J. C.: Conduction of Heat in Solids. Second ed., Oxford Univ. Press, 1959, pp. 491-492.

8. Maslen, Stephen H.: On Heat Transfer in Slip Flow. Jour. Aero/Space Sci., vol. 25, no. 6, June 1958, pp. 400-401.

9. Oman, Richard A., and Scheuing, Richard A.: On Slip-Flow Heat Transfer to a Flat Plate. Jour. Aero/Space Sci., vol. 26, no. 2, Feb. 1959, pp. 126-127.

10. Kennard, E. H.: Kinetic Theory of Gases. McGraw-Hill Book Co., Inc., 1938, p. 327.

NASA-Langley, 1964 E-2586

2/7/80

"The aeronautical and space activities of the United States shall be conducted so as to contribute . . . to the expansion of human knowledge of phenomena in the atmosphere and space. The Administration shall provide for the widest practicable and appropriate dissemination of information concerning its activities and the results thereof."

—NATIONAL AERONAUTICS AND SPACE ACT OF 1958

NASA SCIENTIFIC AND TECHNICAL PUBLICATIONS

TECHNICAL REPORTS: Scientific and technical information considered important, complete, and a lasting contribution to existing knowledge.

TECHNICAL NOTES: Information less broad in scope but nevertheless of importance as a contribution to existing knowledge.

TECHNICAL MEMORANDUMS: Information receiving limited distribution because of preliminary data, security classification, or other reasons.

CONTRACTOR REPORTS: Technical information generated in connection with a NASA contract or grant and released under NASA auspices.

TECHNICAL TRANSLATIONS: Information published in a foreign language considered to merit NASA distribution in English.

TECHNICAL REPRINTS: Information derived from NASA activities and initially published in the form of journal articles.

SPECIAL PUBLICATIONS: Information derived from or of value to NASA activities but not necessarily reporting the results of individual NASA-programmed scientific efforts. Publications include conference proceedings, monographs, data compilations, handbooks, sourcebooks, and special bibliographies.

Details on the availability of these publications may be obtained from:

SCIENTIFIC AND TECHNICAL INFORMATION DIVISION

NATIONAL AERONAUTICS AND SPACE ADMINISTRATION

Washington, D.C. 20546